

Hybrid feedforward-feedback LQR controller based on model prediction for open channel water level control

Xiaohua Li^a, Guanghua Guan^{a,*}, Xin Tian^b, Yufeng Luo^a, Yuequn Huang^c and Jiali Yang^d

^a State Key Laboratory of Water Resources Engineering and Management, Wuhan University, Wuhan 430072, China

^b Dept. of Sustainability and Transitions, KWR Water Research Institute, Groningenhaven 7, Nieuwegein 3433PE, Netherlands

^c Hunan Provincial Water Resources Development & Investment Co., Ltd, Changsha 410007, China

^d Hunan Water Resources and Hydropower Survey, Design, Planning and Research Co., Ltd, Changsha 410007, China

*Corresponding author. E-mail: GGH@whu.edu.cn

ABSTRACT

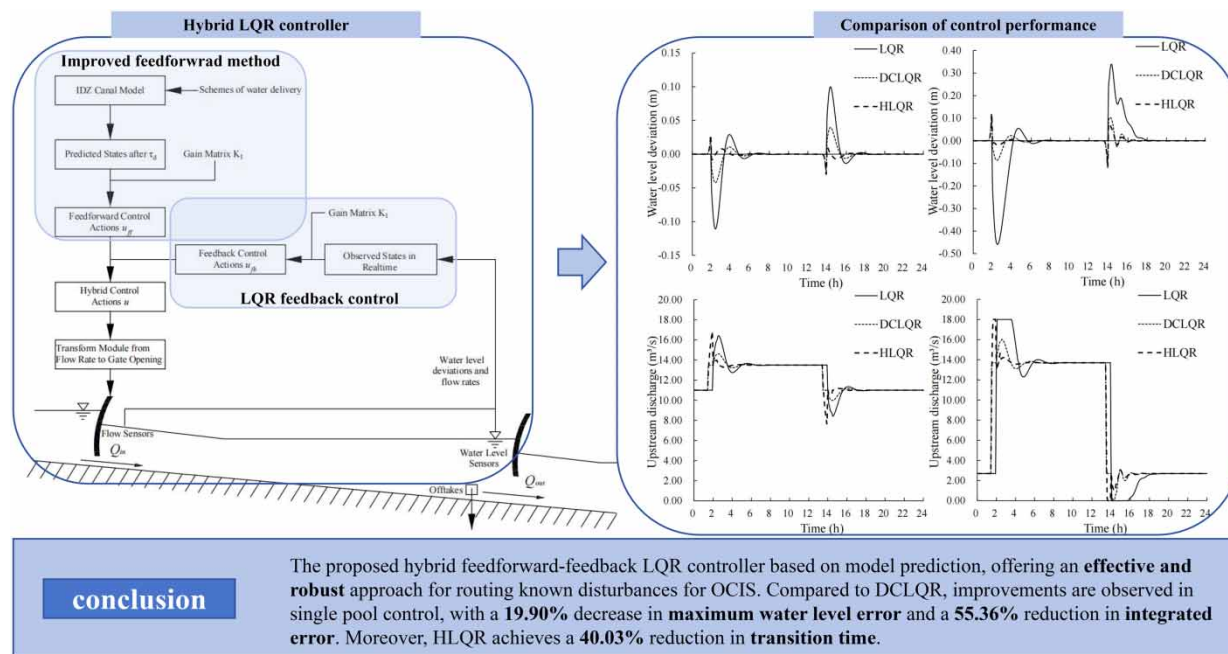
Linear quadratic regulator (LQR), as one of the most popular optimal feedback controllers, has been used in open-channel automatic control. However, existing hybrid feedforward-feedback controllers are simple combinations lacking consistency and neglect the potential of model prediction in the feedforward part. This paper presents a novel hybrid linear quadratic regulator (HLQR) controller with a feedforward-feedback structure. Rather than achieving feedforward control by compensation of discharge or volume, HLQR incorporates a water level prediction of the canal model into the conventional LQR, allowing consistent optimal control and flexible adjustment of weight coefficients in both feedforward and feedback parts. The designed hybrid controller can provide a simple effective way for canal control. It has been numerically tested in a test canal compared with the discharge compensation linear quadratic regulator (DCLQR). Results show that the proposed HLQR can reduce the water level fluctuations and shorten the transition time. The maximum absolute error of the water level can be reduced by 56.65%, the gate movement is decreased by 69.69%, and the transition time is cut down from 21.5 to 7.5 h. With outstanding control performance, the proposed HLQR controller can promote water distribution practically and flexibly, showing great potential in hydraulic control.

Key words: feedforward-feedback structure, hybrid controller, linear quadratic regulator (LQR), model prediction, open channel

HIGHLIGHTS

- A novel hybrid feedforward-feedback LQR controller based on model prediction.
- A simple and effective approach for routing known disturbances in open-channel systems for constant water level control.
- Robust as Manning's n and the coefficient of discharge C_d are untuned.

GRAPHICAL ABSTRACT



1. INTRODUCTION

Securing sufficient water supplies to meet the flexible water demand is always the major task for water distribution systems. Considering the increased food consumption accompanied by the growth of population and the challenge of agricultural water saving, effective automatic control is imperative for open-channel irrigation systems (OCIS) (Godfray *et al.* 2010; Wakamori *et al.* 2020). Current studies increasingly focus on routing demand changes in delivery schedules in OCIS control practice (Garg & Dadhich 2014; Tork *et al.* 2021; Askari Fard *et al.* 2022). With the position adjustment of the outlet structure, the discharges are regulated by each user (Catoni *et al.* 2007). To guarantee the offtakes' flow rate, a constant depth, usually at the downstream end of the pool, is set for each pool of the channel. Therefore, water level control is the key to meeting the changing demands for OCIS. As a remarkable feature of open channels, the time delay can cause difficulties in control as the inflow perturbations can take hours or even days to travel to downstream delivery points (Bautista & Clemmens 2005). An existing challenge is that, when there is an intense outflow change, water levels often fluctuate violently and need a long time to be stabilized due to the time delay.

Feedforward control adjusts outputs in advance based on predicted disturbances, while feedback control corrects errors in real-time by comparing the system's output to the desired value (Dorf & Bishop 2016). To reduce the water level fluctuation and speed up stabilization process for OCIS, many controllers have been developed, of which the control configurations include feedforward, feedback, and a combination of both. Using feedforward controls, the water demand can be met immediately with a small water level deviation due to the moderate water release before the scheduled offtake discharge increases. However, only if the schedule is ideally obeyed with little unknown disturbance and the system model is accurate enough, a perfect control can be achieved simply using feedforward control, which is impractical (van Overloop *et al.* 2008). On the other hand, in feedback, the gate flows are adjusted based on the deviation between the real-time water level and the target level, aiming to regulate the deviation back to zero. In this way, the reduction of disturbances and uncertainties is available (Weyer 2008), which is crucial in practice. Therefore, to leverage the advantages of both feedforward and feedback controls, some literature adopts a hybrid feedforward-feedback configuration (HFFC). By using both together, feedforward reduces deviations before they affect the system, while feedback corrects any remaining errors, making the system more adaptable and improving overall control performance. In open-channel control, Cantoni *et al.* (2007) proposed a feedforward term acting as a 'decoupler' added to the LQR feedback controller. Additional feedforward components in the control loop are described by Aguilar *et al.* (2009) in a predictive control scheme. Shen *et al.* (2009) proposed a model predictive control

(MPC) with feedforward compensation for wastewater treatment improvement. Thus, a well-designed HFFC with both feedforward and feedback controls is necessary for enhanced control performance, and there remains potential for further exploration of HFFC's capabilities.

In the HFFC structure, there is a variety of research on combinations of different control algorithms. For OCIS automatic control, the earliest classical algorithm called proportion-integral-differential (PID) control still holds a dominant position in the industry today and has been revitalized with the help of Artificial Intelligence (AI) technology (Kong *et al.* 2024). Then the linear quadratic regulator (LQR) and MPC have aroused the interest of researchers both with internal model prediction and optimization programming (Conde *et al.* 2021). MPC has rolling optimization and is friendly to constraints that can lead to a satisfactory performance (Zhu *et al.* 2023). Besides, it is noted that MPC takes feedforward along with the feedback into account, while LQR is commonly used only for the feedback gain obtained by the Riccati equation (Conde *et al.* 2021). However, Scokaert & Rawlings (1998) pointed out that constrained LQR achieves significantly better performance than the other forms of MPC on some plants. Moreover, LQRs' performance can be improved with the feedforward methods in the HFFC structure. For example, Yang *et al.* (2020) described a discharge compensation (DC) feedforward strategy for planned water distribution and a linear optimal control method coupled with this strategy responded more quickly and reduced the water level deviations caused by flow imbalance. However, whether using the DC method or volume compensation (VC) method (Bautista & Clemmens 2005), the feedforward logic is disconnected from feedback control, so it cannot be optimized under a unified objective function for weight allocation. In previous studies on feedforward control methods for OCIS, model-based optimization has rarely been used. Instead, feedforward actions are typically derived based on compensation principles of discharge and water volume as mentioned. There have been studies using model-based optimization for OCIS through MPCs (Horváth *et al.* 2015; Aydin *et al.* 2017). But in MPC, the feedforward component is not separated but instead unified with the feedback control in a one-objective function optimization. However, the requirements for the transition process in feedforward and feedback control are often different, which means that using a single objective function for optimization cannot meet the flexible control needs with phased objectives. Therefore, there is still a lack of exploration on the flexibility of weight allocation and consistency of HFFC between the feedforward and feedback components.

Focusing on LQR controllers, current research highlights the significant advantages of LQR in offering optimality over an infinite horizon. However, to the best of the authors' knowledge, the model prediction-based linear optimization of LQR has not been utilized in feedforward control for OCIS. Classical LQR is presented for feedback control problems, with some researchers adding feedforward controls to enhance performance, but few have considered to use prediction-to-optimization control logic in feedforward, which may contribute to a consistent hybrid structure and performance improvements. Therefore, this study's primary objective is to introduce an improved hybrid controller called the hybrid linear quadratic regulator (HLQR), combining model prediction and optimal control in a consistent HFFC that allows flexible weight allocation. This approach aims to generate an alternative controller with smaller deviations and shorter transition times for constant water level control under known disturbances.

The paper is structured as follows. Section 2 introduces the linear canal model (Section 2.1) and basic LQR feedback controller (Section 2.2) and then presents the model-based feedforward control (Section 2.3) and HLQR controller structure (Section 2.4), followed by the control architecture (Section 2.5). The information of the case study is provided in Section 3, and results are shown in Section 4 and discussed in Section 5. Finally, the conclusions are drawn in Section 6.

2. CONTROLLER DESIGN

2.1. Linear canal model

LQR control requires a linear model describing the control object, and the model accuracy is the key factor in feedforward and largely decides the controller performance (Litrigo & Fromion 2009; Vorosmarty *et al.* 2010; Askari Fard *et al.* 2021). The Saint-Venant equations (SVEs) are a set of non-linear partial derivative equations that describe the flow dynamics for open channels (Cunge *et al.* 1980; Litrigo & Fromion 2006). As appropriate simplifications derived from the Navier-Stokes equations, the SVEs have been the most commonly used mathematical tool for modeling open channels and rivers (Kurganov & Levy 2002; Gerbeau & Perthame 2021). Considering the SVE are partial derivative equations, which are not easy to deal with for control, a classical way is to apply the linear models (Rabbani *et al.* 2009). In this study, a first-order linear canal model called the integrator delay zero (IDZ) model is used. Proposed by Litrigo & Fromion (2004a),

the IDZ model has an integrator and a delay in low frequencies and models the high frequencies by a constant gain and a delay. It can provide a frequency domain representation of SVEs in any flow configuration (Litrice & Fromion 2004b).

The integrator part has a gain that is inversely proportional to the backwater area (A_s). The delay ($\Delta\tau$) is the time for the transfer between upstream discharge (q_i) and downstream level (h_2) (Figure 1). Besides, the IDZ model includes an IDZ approximation of transfer z_1 and an integrator zero approximation of transfer z_2 , leading to the frequency domain model:

$$h_i = \frac{1 + z_1 s}{A_s s} e^{-\Delta\tau s} q_i - \frac{1 + z_2 s}{A_s s} (q_{i+1} + q_{\text{off},i}) \quad (1)$$

where q_{i+1} is the downstream check gate discharge; and the $q_{\text{off},i}$ is the offtake discharge as the offtakes located at the downstream end.

The water level error e_i can be written as the difference between the actual water level h_i and the setpoint h_{set} , that is

$$e_i = h_i - h_{\text{set}} \quad (2)$$

where i is the pool number.

Thus, the control objective is to keep e around zero, and the control variable is q by adjusting the check gate. From this perspective, by discretizing Equation (1), a state-space model for a canal pool can be constructed in the following form:

$$\begin{cases} \mathbf{x}(k+1) = \mathbf{A}\mathbf{x}(k) + \mathbf{B}\mathbf{u}(k) \\ \mathbf{y}(k) = \mathbf{C}\mathbf{x}(k) + \mathbf{D}\mathbf{u}(k) \end{cases} \quad (3)$$

where \mathbf{x} is the state variable, \mathbf{u} is the control variable, \mathbf{A} is a $n \times n$ square matrix, where n is the dimension of vector \mathbf{x} , \mathbf{B} is a $n \times 1$ matrix, \mathbf{y} is the output variable standing for water level deviation at downstream end, \mathbf{C} is a $1 \times n$ square matrix, \mathbf{D} is a 1×1 matrix. Note that matrices \mathbf{A} and \mathbf{B} are determined by the linear model representing the dynamic characteristic, while matrices \mathbf{C} and \mathbf{D} are determined by controller design.

The canal pool state contains the water level error and the discharge at the present instants, and discharges all the instants during the delay time:

$$\mathbf{x}(k) = [e(k) \quad q(k - k_\tau) \quad q(k - k_\tau + 1) \quad \dots \quad q(k - 1) \quad q(k)]^T \quad (4)$$

where i is the pool number, $k = \text{round}\left(\frac{\tau_d}{DT}\right)$, is the number of delayed time steps.

The control variable $\mathbf{u}(k)$ is given by

$$\mathbf{u}(k) = q(k) \quad (5)$$

where $q(k)$ is the upstream discharge, m^3/s .

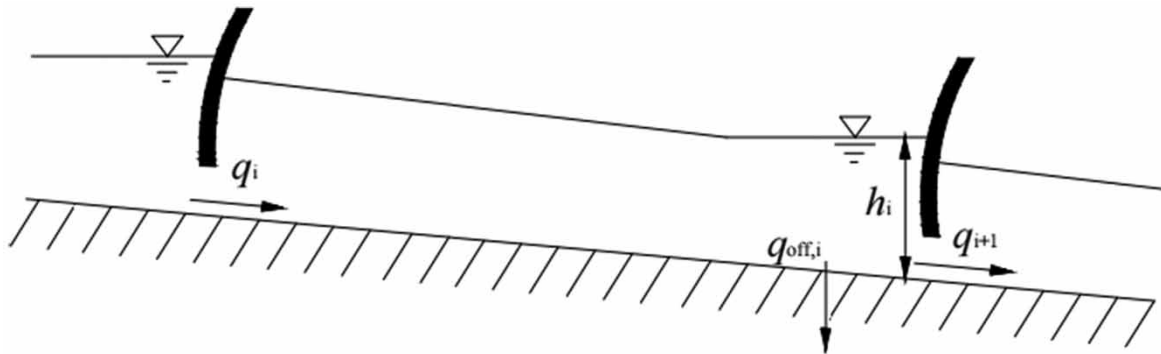


Figure 1 | Scheme of a canal pool.

The output variable contains the downstream water level deviations of pools, given by

$$\mathbf{y}(k) = \mathbf{e}(k) \tag{6}$$

For multi-pool channels:

$$\mathbf{x} = [\mathbf{x}_1, \mathbf{x}_2, \dots, \mathbf{x}_N]^T, \mathbf{y} = [\mathbf{y}_1, \mathbf{y}_2, \dots, \mathbf{y}_N]^T, \mathbf{u} = [\mathbf{u}_1, \mathbf{u}_2, \dots, \mathbf{u}_N]^T \tag{7}$$

That is

$$\mathbf{x} = \begin{bmatrix} e_1(k) & q_1(k - k_{\tau,1}) & q_1(k - k_{\tau,1} + 1) & \dots & q_1(k - 1) & q_1(k) \\ e_2(k) & q_2(k - k_{\tau,2}) & q_2(k - k_{\tau,2} + 1) & \dots & q_2(k - 1) & q_2(k) \\ \dots & \dots & \dots & \dots & \dots & \dots \\ e_N(k) & q_N(k - k_{\tau,N}) & q_N(k - k_{\tau,N} + 1) & \dots & q_N(k - 1) & q_N(k) \end{bmatrix}^T \tag{8}$$

$$\mathbf{y} = [e_1(k), e_2(k), \dots, e_N(k)]^T \tag{9}$$

$$\mathbf{u} = [q_1(k), q_2(k), \dots, q_N(k)]^T \tag{10}$$

This model provides the relationship between the downstream water level and the discharges both upstream and downstream. Although the actual actuators are the check gates, this study sets the gate discharge, rather than the gate opening, as the control variable. Because the relationship between flow rate and gate opening is non-linear (Clemmens *et al.* 2003), choosing flow changes makes it possible to keep the linear relationship between system states and control variables in the state-space equation accurately and helps avoid local gate control errors and calibration errors in the flow formula.

2.2. LQR feedback controller

This paper uses the theory of LQR optimal control to design the feedback part of the controller that regulates the upstream gate discharge based on the deviation of the downstream water level of each pool in an open-channel system. The control aim is to keep a constant downstream water level to guarantee the water supply (Malaterre 2008). The control formulation is to get the proper series of control variable u , which is designed to regulate $\mathbf{e}(k) \rightarrow 0$ as $k \rightarrow \infty$ with the minimal objective function

$$J = \sum_{k=0}^{\infty} \mathbf{x}(k)^T \mathbf{R}_x \mathbf{x}(k) + \mathbf{u}(k)^T \mathbf{R}_u \mathbf{u}(k) \tag{11}$$

where \mathbf{R}_x is the cost of water level deviation; \mathbf{R}_u is the cost of control action.

Referring to previous literature, the objective function in this study includes two factors: water level deviations and discharge changes. The first term of the objective function measures the accumulation of water level fluctuations during the system's transition process, while the second term assesses the cumulative changes in flow rate, which essentially represent the accumulation of gate-position actions since the discharges are controlled by check gates. This ensures that the output variables can approach zero with the minimal total cost of water level fluctuations and gate-position adjustments. Operators can allocate the cost weights of both factors according to specific control objectives and management preferences.

Hence the physical control problem defined by Equations (3) and (7) can be formulated in an LQR framework (Balogun *et al.* 1998), and the optimal sequence of feedback control is given by

$$\mathbf{u}(k) = -\mathbf{K}\mathbf{x}(k) \tag{12}$$

in which the constant feedback gain matrix \mathbf{K} is given by

$$\mathbf{K} = \mathbf{R}^{-1} \mathbf{B}^T \mathbf{S} \tag{13}$$

and \mathbf{S} is the single positive definite solution of the Riccati equation:

$$\mathbf{S}\mathbf{A} + \mathbf{A}^T \mathbf{S} + \mathbf{Q} - \mathbf{S}\mathbf{B}\mathbf{R}^{-1} \mathbf{B}^T \mathbf{S} = 0 \tag{14}$$

2.3. Improved feedforward controller

In the improved feedforward (ImpFF) controller, the scheduled demand changes of water intakes are input into the IDZ model, and the water level deviations can be predicted as the output of the model. Then, the future water level predicted by the canal model is used along with the gain matrix of LQR for optimal feedforward control action. Specifically, by multiplying the water level deviation after delay time e_{k_τ} and the gain matrix K_1 of the LQ problem, the optimal solution u_{ff} is obtained for feedforward control (Equation (11)). In this way, the control action of the upstream gate at time t is obtained in advance based on predicted downstream water level deviations at time $t + \Delta\tau$. After that, the states of the next step can be predicted, and the corresponding feedforward actions can be obtained based on the updated states, to make a circle. The calculation process is as follows:

$$e_{k_\tau} = -\frac{1 + z_2 S}{A_s S} q_{\text{off},s} \tag{15}$$

$$\mathbf{x}_0 = [e_{k_\tau} \ 0 \ 0 \ \dots \ 0 \ 0]^T \tag{16}$$

$$\mathbf{u}_{ff,i} = -\mathbf{K}_1 \times \mathbf{x}_i \tag{17}$$

$$\mathbf{x}_{i+1} = \mathbf{A}\mathbf{x}_i + \mathbf{B}\mathbf{u}_{ff,i} \tag{18}$$

where e_{k_τ} is the prediction of water level deviation after k_τ steps (m); u_{ff} is actions of feedforward (m^3/s); i is the number of time step, $i = 0, 1, 2, 3, \dots$

The key innovation of this feedforward method is its use of predicted future deviations instead of present states, in combination with the LQR control law, to determine the feedforward actions. This approach integrates canal model prediction with optimal control to create a feedforward controller, which contrasts with conventional LQR controllers that primarily rely on feedback using real-time states.

2.4. HLQR controller structure

Based on the linear canal model and the LQR algorithm, the control laws in matrix form are obtained in Figure 2. Then, a hybrid feedforward-feedback LQR controller is designed as shown in Figure 3, aiming at minimizing the water level deviation and the flow rate changes during the offtake flow change process and regulating the water level to the setpoint.

The HLQR comprises two parts: the feedforward component and the feedback component, differing in two aspects. Firstly, the input in the feedforward is predicted based on future schemes of water delivery, whereas the input in the feedback is derived from real-time observation data. Secondly, the objective function may vary between the two LQ problems: for the feedforward controller, it typically addresses large deviations, while for the feedback controller, it is more adapted to small deviations. Within the hybrid structure, the feedforward component is designed to address water level discrepancies resulting from anticipated flow changes, whereas the feedback component aims to mitigate real-time discrepancies

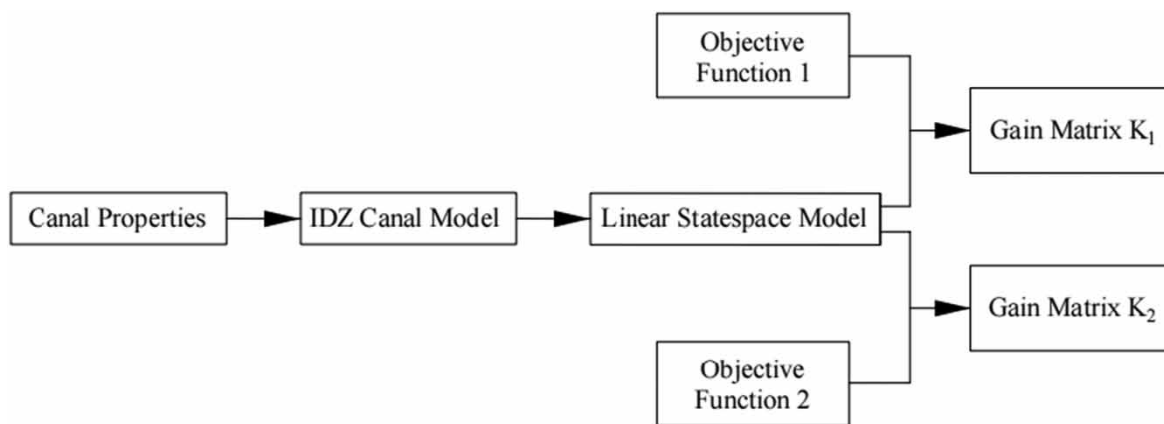


Figure 2 | Gain matrixes obtained by LQR algorithm based on IDZ model.

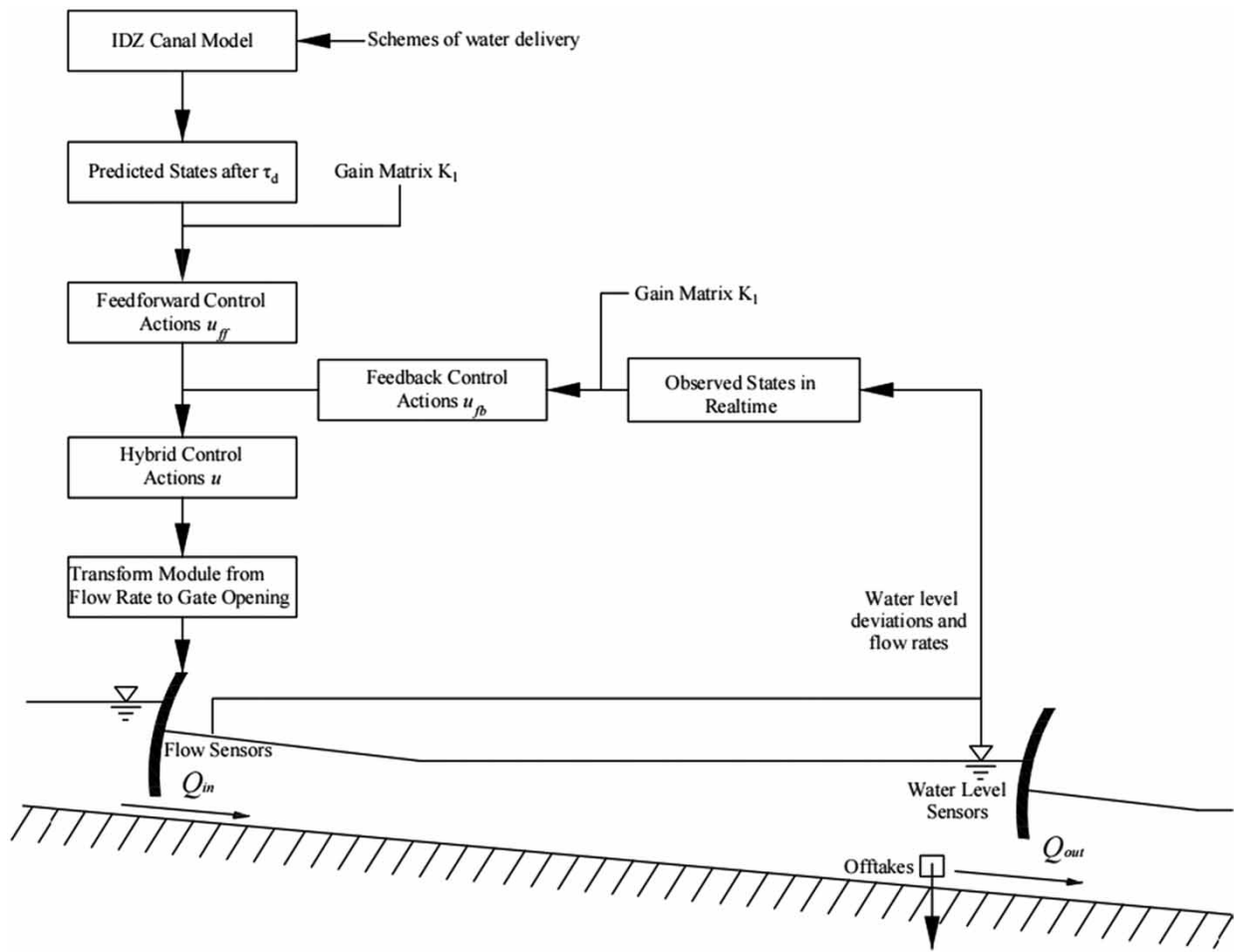


Figure 3 | Structure of the HLQR controller in a canal pool.

arising from other factors during operation, such as model errors, monitoring inaccuracies, uncertain flow variations, and so forth.

In the proposed hybrid controller, both the feedforward and feedback controllers remain open throughout the control process. However, their roles differ: the feedforward controller operates solely during the delay period preceding a scheduled discharge change, while the feedback controller remains operational continuously to address any water level discrepancies. For instance, if a scheduled demand change occurs at 10:00 with a 30-min pool delay, the feedforward controller initiates at 9:30 and ceases at 10:00, whereas the feedback controller remains active to counteract unknown disturbances at any time. It's important to note that the control processes of the feedforward and feedback parts do not have conflicting control commands at the same time; instead, they are sequentially connected in different periods. The feedforward actions are tailored to manage anticipated flow changes and are active only before the scheduled change begins. Conversely, the feedback component handles unforeseen flow variations and water level discrepancies caused by operational errors, operating throughout the entire control process.

For a canal pool, real-time observations of downstream water level and upstream flow rate are obtained via sensors and updated at each time step to reflect the system's current state. Subsequently, the feedback control action u_{fb} is computed by

$$u_{fb} = -K_2 \times e \tag{19}$$

So, the actual upstream discharge change is given by

$$\mathbf{u} = \mathbf{u}_{ff} + \mathbf{u}_{fb} \quad (20)$$

Combining the ImpFF method with classical LQR feedback control, the final control actions are determined by Equation (14). To adjust the gate operations, the subsequent step involves converting the inflow actions into gate openings and implementing them based on the anticipated delay time of each pool. Moreover, the gate opening is calculated in reverse using the gate discharge formula utilized in the Central Arizona Project in the United States (Dent 2004).

$$q = C_d G b \sqrt{2g(y_u - y_d) + \frac{q^2}{A_u^2}} \quad (21)$$

where q is the check gate discharge (m^3/s); C_d is the discharge coefficient; G is the gate opening (m); b is the gate width (m); $g = 9.81$, is the gravitational acceleration (m/s^2); y_u and y_d are the water level upstream and downstream side of the gate (m); and A_u is the wetted area upstream of the gate.

2.5. Control architecture

In this paper, a centralized architecture is adopted for multi-pool canals. The multi-cascade pools are interconnected in the state space (Equations (3)–(6)). Centralized control entails declaring all input and output variables of the system as vectors within a single equation, with control actions generated by a central controller (Malaterre 1995; Hashemy Shahdany *et al.* 2019). In the proposed controller, with a unified function J , all pools are encompassed within one state space, i.e., $\mathbf{x} = [\mathbf{x}_1, \mathbf{x}_2, \dots, \mathbf{x}_N]^T$, $\mathbf{y} = [\mathbf{y}_1, \mathbf{y}_2, \dots, \mathbf{y}_N]^T$, $\mathbf{u} = [\mathbf{u}_1, \mathbf{u}_2, \dots, \mathbf{u}_N]^T$. Model predictions and control actions for the multi-pool system are provided by the multiple-input multiple-output (MIMO) state-space model based on the IDZ model. For cascaded channels, the delay time of each gate should be considered, accounting for the pools from the offtake to the gate.

In typical OCIS, a constant depth is the control aim in each pool, and water is delivered to users through outlet structures. In this study, a control mode known as distant downstream water level control is employed. The objective of this control mode is to uphold a consistent water level downstream of the pool by regulating the upstream check gate and the flow passing through it. Regarding distant downstream control, Malaterre (1995) highlights that there are no inconveniences with the slope of the channel, reducing construction costs.

3. CASE STUDY

3.1. Test canal

The test case is the Test Canal 2 developed by the Task Committee on Canal Automation Algorithms of the American Society of Civil Engineers (ASCE) (Clemmens *et al.* 1998). Figure 4 depicts the basic parameters of the test canal. The upstream boundary of the canal system consists of a reservoir with a constant water level, while the end gate serves as the downstream boundary condition with a fixed flow rate. The water intake is located near the downstream end of the pool (50 m to the downstream gate). That is, the discharge of the intake $Q_{\text{off},i}$ and the discharge through the downstream gate Q_{i+1} have similar effects on the water level at the downstream end, which is the assumption of the IDZ model. According to the work of Clemmens *et al.* (1998) and Litrico & Fromion (2004c), the IDZ model parameters and physical parameters of the canal are detailed in Appendix Tables A1–A3.

3.2. Test scenarios

The presented feedforward method ImpFF is compared with the simple discharge compensation feedforward (DCFF) method in an open-loop control test that a $2.5 \text{ m}^3/\text{s}$ scheduled downstream flow change occurs at 2 h. The proposed HLQR controller undergoes testing in both a small-flow change and a large-flow change within a single pool compared with the discharge compensation linear quadratic regulator (DCLQR) (Zhong *et al.* 2020). Pool 1 of the test canal depicted in Figure 4 is selected for the single-pool tests (Test 1-1 and Test 1-2), with the settings detailed in Table 1. Subsequently, the designed controller, employing a centralized architecture, is numerically applied to the ASCE Test Canal 2 in a multi-pool assessment. Its performance is then compared with a recently introduced LQR controller utilizing a pure discharge feedforward method (Zhong *et al.* 2020) that achieves feedforward control according to the delay time by compensating for the discharge at offtake.

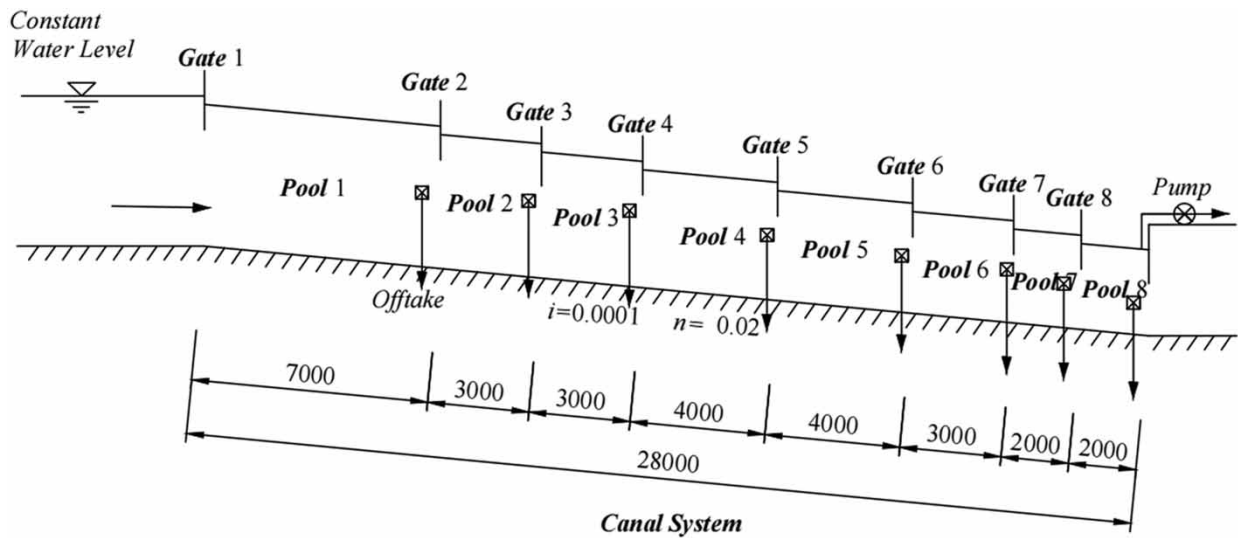


Figure 4 | Physical parameters of the ASCE Test Canal 2.

Table 1 | Small-flow change scenario 1-1 and large-flow change scenario 1-2 of Test 1

Scenario number	Initial upstream flow (m ³ /s)	Initial downstream flow (m ³ /s)	Scheduled downstream flow change at 2 h (m ³ /s)	Scheduled downstream flow change at 14 h (m ³ /s)
1-1	11.0	11.0	+2.5	-2.5
1-2	2.7	2.7	+11.0	-11.0

Additionally, tests assessing the robustness of the HLQR controller are conducted with untuned Manning n and gate discharge coefficient C_d values.

Both Test 1-1 and Test 1-2 involve scheduled flow changes at the downstream end. The former flow change is 2.5 m³/s, while the latter is 11 m³/s. Three controllers are employed, each utilizing the same LQR control in feedback, while employing no method, DC method, and ImpFF method in feedforward, respectively, for Test 1-1 and Test 1-2. In practice, control objectives encompass multi-pool canal systems. Test 2-1 is conducted on the ASCE Test Canal 2, comprising an eight-pool canal system. The flow changes in Test 2-1 (Table 2) reference the scenario presented by Clemmens *et al.* (1998). To allow adequate time for feedforward control, water intake channels are uniformly set at the end of the second hour after simulation commencement.

Table 2 | Multi-pool scenario 2-1 of Test 2

Pool number	Initial upstream flow (m ³ /s)	Initial flow of offtakes (m ³ /s)	Scheduled flow of offtakes after 2 h (m ³ /s)	Resulting upstream flow (m ³ /s)
1	11	1	1	13.5
2	10	1	1	12.5
3	9	1	1	11.5
4	8	1	1	10.5
5	7	1	2.5	9.5
6	6	1	2	7
7	5	1	1	5
8	4	1	1	4

To assess the robustness of the proposed HLQR controller, two untuned parameters are deliberately set with deviations from their known values. The gate discharge coefficient C_d is crucial for controlling the actual gate discharges in the execution of the control algorithm as mentioned in Equation (15). Similarly, roughness n , as an important parameter to characterize open-channel flow-water level relationship, greatly affects the accuracy of model predictions (Liu *et al.* 2024). Using biased hydraulic parameters (n and C_d) in the predictive model for control, the scenarios in Test 2 have been repeated. Specifically, the Manning n is 0.020 for the controller and 0.024 for the simulation, which is increased by 20%. And gate discharge coefficient C_d is 0.83 for the controller and 0.996 for the simulation increasing by 20%.

3.3. Performance indicators

The primary goal for OCIS is to distribute the correct quantity of water to each user within a specified timeframe (Weyer 2008). To demonstrate the control system's performance during the transition process, a selection of indicators has been designated numerically (Clemmens *et al.* 1998; Guanghua *et al.* 2018). Maximum absolute error (MAE) and integral of the absolute magnitude of error describe the control level of water level, while nondimensional integrated absolute discharge change (NIAQ) and nondimensional integrated absolute gate movement (NIAW) indicate the fluctuation of the flow rate and accumulation of gate action as they are highly correlated by gate discharge formulation. The transition time T_{tran} serves to characterize the stabilization speed of the controller, which is crucial for effective canal system management. Prolonged transition times can result in system instability and operational hazards, such as overflows.

Performance indicators:

$$\text{MAE} = \frac{\max(|y_t - y_{\text{target}}|)}{y_{\text{target}}} \quad (22)$$

$$\text{IAE} = \frac{\frac{\Delta t}{T} \sum_{t=0}^T |y_t - y_{\text{target}}|}{y_{\text{target}}} \quad (23)$$

$$\text{NIAQ} = \frac{\frac{\Delta t}{T} \left(\sum_{t=t_1}^{t_2} |Q_t - Q_{t-\Delta t}| - |Q_{t_1} - Q_{t_2}| \right)}{Q_{\text{design}}} \quad (24)$$

$$\text{NIAW} = \frac{\frac{\Delta t}{T} \left(\sum_{t=t_1}^{t_2} |W_t - W_{t-\Delta t}| - |W_{t_1} - W_{t_2}| \right)}{W_{\text{max}}} \quad (25)$$

$$T_{\text{tran}} = t_2 - t_1 \quad (26)$$

where t_1 is the time when flow change happens, and t_2 is the time when the system is stable.

Note that in this study, the stable state is defined as the water level deviation is no more than 2% of the target depth, and gate opening changes of no more than 0.005 m.

These four nondimensional indicators (Equations (16)–(20)) have been selected to cover different aspects for a single pool, including the water level, discharge, gate opening, and transition time. For multi-pool canal systems, MAE and T_{tran} is the largest value across all pools, while the other five indicators are averaged.

3.4. Simulation settings

The hydrodynamic calculation platform (Wang & Guan 2011) is used to simulate the one-dimension dynamic process of water in the canal, programmed in MATLAB. In this software, a Preissmann implicit scheme difference method has been used to solve the SVEs. The simulation time step (ST) of solving the SVEs, as the simulation interval, matters in the simulation result. A smaller ST produces a more precise process with many spots on the chart and allows the controller to take a smaller discrete control time step (DT) to make a more sophisticated control with accurate delay-time steps and control timings. DT must be a positive integer multiple of ST. Otherwise, the control action may fall in the simulation time step and be unable to execute on time. To avoid too frequent gate adjustments, the DT cannot be too small in practice. Different ST and DT have been set according to the test scenarios. DT is 5 min in Test 1 for precise numerical simulation and 15 min in Test 2-1 for

consistency with the comparative case (Zhong *et al.* 2020). The total simulation time is 24 h for the single pool in Test 1 and 72 h in Test 2-1. The deadband is set to zero in this study. ST is related to the precision of the simulation results. Considering the complexity of the simulation channel, the water intake disturbances, and the completeness of the result curves, we determined, by trial and error, that ST is set to 5 min both in Test 1 and in Test 2-1. It should be noted that control actions are moved to the closest flow control interval (Clemmens *et al.* 2010). For example, the offtake demand is scheduled to increase at 10:30 at the end of the pool, while the IDZ model delay is 28.9 min. Then the upstream check gate should increase the flow at 10:01. But no action is taken during the interval ST. So, the flow control would begin at 10:00, which may cause some timing errors. Nonetheless, with a 5-min interval, these errors are negligible.

Cost weighting coefficients play a crucial role in determining control bias. Current research typically employs constant matrices for \mathbf{Q} and \mathbf{R} , determined through trial and error (Clemmens & Schuurmans 2004; Clemmens & Wahlin 2004). Operators have the flexibility to assign different weighting values for each canal pool and gate. In this study, following the principle of water level priority, the weight of the water level deviation needs to be larger than that of the control cost (cumulative flow variation). So, the weight matrix sets \mathbf{R} as the unit diagonal matrix and \mathbf{Q} as 1,000 times \mathbf{R} in the feedback objective function to reduce steady-state deviation. On the other hand, the ratio (\mathbf{Q}/\mathbf{R}) in the feedforward component is set to 100, to avoid excessive overshoot. The initial system condition for LQR control involves a steady flow with no downstream water level deviations, thereby necessitating no feedback actions at the onset of the simulation.

4. RESULT

4.1. Open-loop control

The open-loop test shown in Figure 5 indicates the differences between DCFE and ImpFF. As shown in Figure 5(a), before the water intake disturbance occurs, both DCFE and ImpFF proactively control the upstream gate flow in advance. DCFE adjusts the flow to the required level where upstream and downstream flows are equal and then maintains it, while ImpFF makes a larger adjustment and returns to the required flow level at the time of the disturbance. By observing the corresponding changes in the flow and water level processes, it can be inferred that the additional adjustment by ImpFF, exceeding the required flow, results in a smaller maximum deviation and a lower steady-state error in the downstream control point water level. The underlying reason may be that the shape of the water wave attenuates as it propagates downstream. For instance, in Figure 5(b), the increased upstream flow of $2.5 \text{ m}^3/\text{s}$ forms a rising wave that attenuates as it moves downstream, resulting in a smaller increase in water level at the downstream end than a corresponding decrease caused by a $2.5 \text{ m}^3/\text{s}$ downstream flow reduction falling wave. The damped rising wave counters the unattenuated falling wave, leading to a drop in water level (see Figure 5(a)). Conversely, the overshoot in Figure 5(c) is the result of an attenuated falling wave counteracting an unattenuated rising wave.

4.2. Single-pool control

The results of single-pool control are shown in Figure 6 in Test 2. The designed HLQR controller demonstrates satisfactory performance, with the water level maintained around the target level in response to changes in users' demand. Initially, the water level aligns with the setpoint, resulting in zero deviation at the outset. However, due to the increase in outflow downstream, the water level experiences a sharp decline, reaching its lowest point. Subsequently, it oscillates several times before gradually stabilizing around the setpoint.

In Figure 6(a), the maximum absolute value of water level deviation of HLQR is under 0.03 m, which is smaller than that of DCLQR (around 0.05 m) and LQR (more than 0.10 m). Moreover, the water level deviation of HLQR returns to zero faster, responding to the shortest transition time among these three controllers. Notably, HLQR, similar to DCLQR, leads to an increase in upstream discharge (Figure 6(b)) and a slight increase in water level before the scheduled flow change at the end of 2nd hour. It shows that the feedforward part of control generates an inflow release, which is preparing for the outflow increase and minimizing the deviation around, unlike the big drop in the water level of LQR without any feedforward. Benefiting from the feedforward actions, the subsequent oscillations of both HLQR and DCLQR are smaller and the water level deviations approach faster to zero, despite the identical feedback components of the three controllers. As shown in Figure 6(b) and 6(c), the upstream discharge of HLQR is greater than that of DCLQR in the first peak and has a weaker fluctuation after the peak. It can be seen that, in Figure 6(b) and 6(e), the upstream discharge of each pool has an overshoot, which may be a weakness of this controller. If this LQR feedforward controller is used alone, steady-state water level deviation will be unavoidable. Therefore, it is essential to design a hybrid controller for sound control. The gate-opening processes have the same

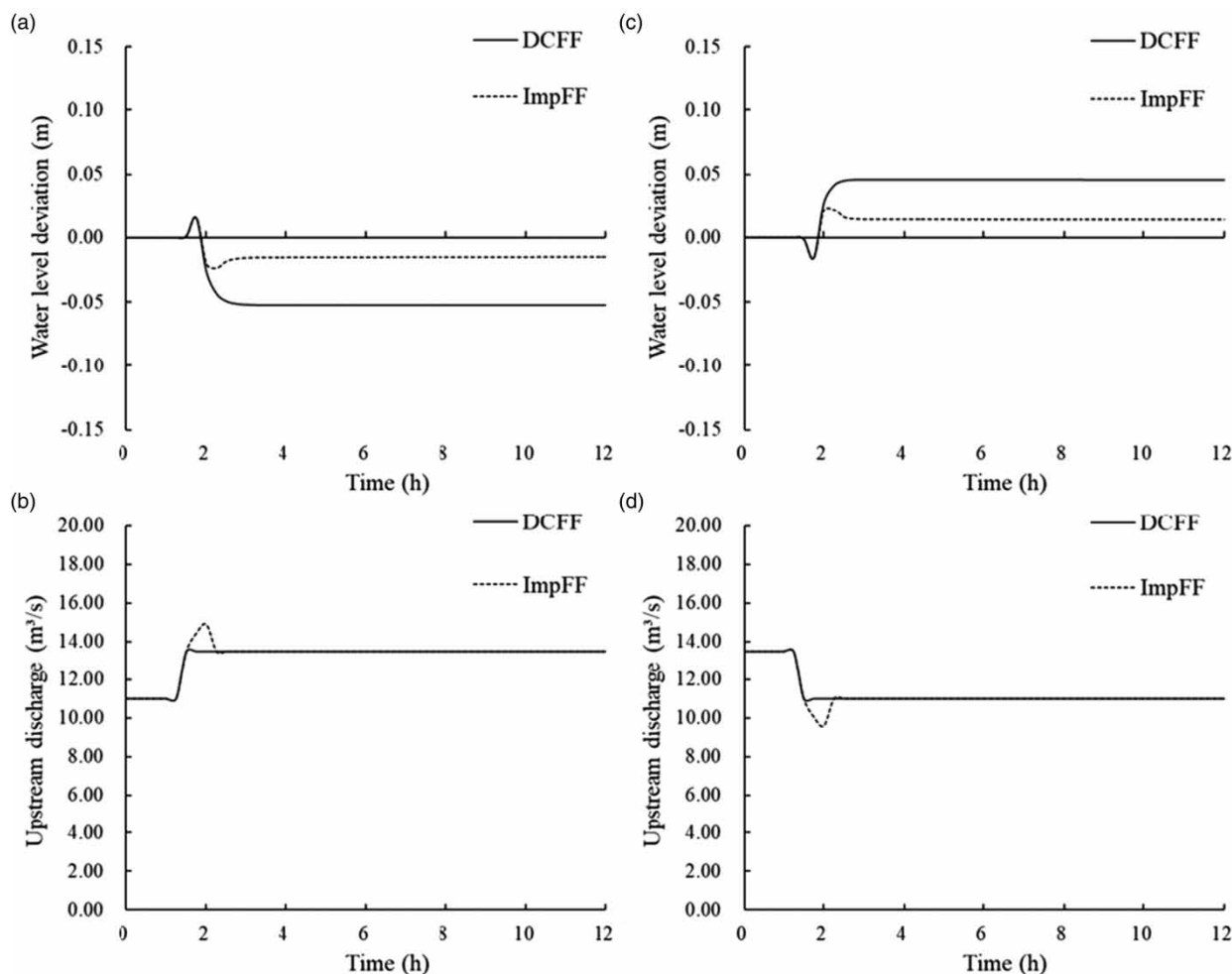


Figure 5 | Open-loop control in small-flow change: (a) and (c) for water level deviation; (b) and (d) for upstream discharge.

trend as the discharges, as the discharge and opening of a gate are strictly positively corresponded by the gate flow formula. Overall, the HLQR controller shows the best performance with the smallest water level deviation (the absolutes are less than 0.03 m) and the shortest transition time during the regulation process.

The performance indicators for scenario 1-1 are summarized in Table 3. Upon examining the overall performance, it becomes evident that both HLQR and DCLQR exhibit significant improvements with feedforward. Furthermore, they each possess advantages in different aspects. Specifically, DCLQR demonstrates less accumulation of discharge changes and gate-position adjustments compared to HLQR, which effectively controls water level deviations to a lower level. Interestingly, they utilize the same parameters in Q and R , suggesting that the difference in tradeoff between water level deviations and flow changes is likely attributable to feedforward control. In other words, the proposed HLQR achieves better water level control with smaller maximum and integral deviations but incurs greater adjustments in discharge and gate opening. Regarding transition time, DCLQR and HLQR exhibit times of 130 and 85 min, respectively, representing a notable 35% reduction crucial for canal system control. Overall, a significant improvement is observed in water level control and transition speed, positioning HLQR as a viable alternative for canal control as a hybrid controller.

Similar trends are observed in the large-flow change scenario Test 1-2 (Figure 6(d)). Under both DCLQR and HLQR control, water levels exhibit rises before the offtake discharge change at the end of the second hour due to feedforward control, while LQR maintains the initial water level without feedforward. Subsequently, all three water levels experience sharp drops of varying magnitudes followed by increases due to the feedback controller, ultimately returning to zero deviation. It's important to note that the control variables, upstream discharges, reached the maximum ($18 \text{ m}^3/\text{s}$) and minimum ($0 \text{ m}^3/\text{s}$) values in

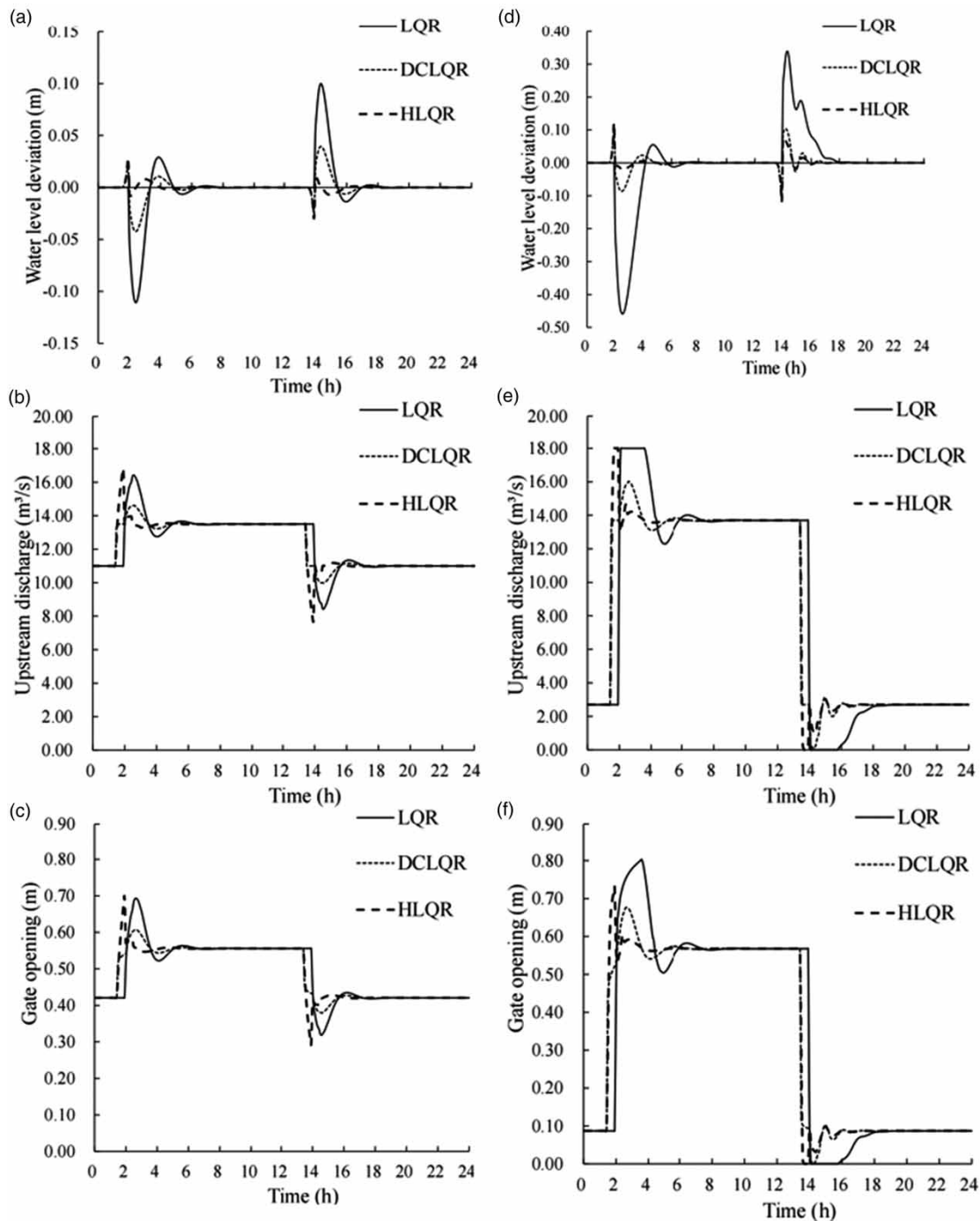


Figure 6 | Single-pool control performance in small-flow change scenario 1-1 and in large-flow change scenario 1-2: (a) and (d) for water level deviation; (b) and (e) for upstream discharge; (c) and (f) for gate opening.

Test 1-2. Therefore, the water level control is influenced by discharge constraints. Figure 6(d) underscores the importance of feedforward control under large-flow change conditions, as pure feedback LQR results in significant water level deviation (exceeding -0.45 m) and extreme discharges approaching limiting values, posing risks to operational safety. In contrast, both DCLQR and HLQR exhibit milder water level deviations and shorter periods of extreme discharges compared to pure LQR control. Regarding transition time to the stable state, HLQR achieves the shortest duration of 90 min,

Table 3 | Control performance of the single pool in scenario 1-1

Feedforward method	Flow change (m ³ /s)	MAE ($\times 10^2$)	IAE ($\times 10^3$)	NIAQ ($\times 10^3$)	NIAW ($\times 10^4$)	Transition time (min)
LQR	2.5	5.28	5.23	2.61	8.03	190
DCLQR	2.5	2.02	2.10	1.47	4.08	130
HLQR	2.5	1.15	1.15	3.49	8.42	85

Note: $y_{\text{target}} = 2.1$ m, and $Q_{\text{design}} = 14$ m³/s and the full gate opening is 2.3 m for pool 1 and more details are shown in Appendix Table A1.

approximately one-third of LQR's longest duration (270 min), while DCLQR falls in the middle with 165 min. The performance indicators in Test 1-2, as listed in Table 4, consistently highlight the superiority of feedforward control across all five aspects. In comparison between DCLQR and HLQR, the latter shows faster stabilization speed with smaller water level deviation, while the former exhibits less accumulation of discharge changes and fewer gate adjustments.

Overall, the presented HLQR controller achieves a smaller overshoot and a shorter transition time, owing to the enhanced feedforward method and well-matched hybrid design of feedforward and feedback. However, it incurs greater gate adjustments, potentially accelerating ageing and increasing energy consumption.

4.3. Multi-pool control

The result shows (Figure 7) that the deviations are in or slightly beyond the range of -0.03 to 0.04 m, proving the effectiveness of the proposed controller. Additionally, the control actions show a smooth process in discharge with a small overshoot (around 1.0 m³/s), affirming the stability of HLQR. When viewed individually for each pool, Pool 1 experiences the earliest change in water level and takes the longest to return to zero deviation. Conversely, Pool 6 exhibits the shortest fluctuation time, while Pools 7 and 8 are almost unaffected by the changes.

Overall, the proposed HLQR controller demonstrates satisfactory performance compared to DCLQR. The HLQR controller exhibits a 56.65% reduction in MAE, a 69.69% reduction in gate-opening accumulation, and a 65.12% reduction in transition time (Table 5). It is noteworthy that while the proposed HLQR controller results in more gate actions in the single-pool test, it leads to fewer gate actions in the multi-pool test. One possible explanation is that HLQR can stabilize the pool in a shorter time than DCLQR, as demonstrated in Figure 7, with less gate actions. For the tested 8-pool canal, DCLQR requires considerably more time to stabilize the system compared to HLQR. During the transition period,

Table 4 | Control performance of the single pool in scenario 1-2

Feedforward method	Flow change (m ³ /s)	MAE ($\times 10^2$)	IAE ($\times 10^3$)	NIAQ ($\times 10^3$)	NIAW ($\times 10^4$)	Transition time (min)
LQR	11	21.86	26.70	6.08	19.22	270
DCLQR	11	5.51	4.81	3.09	8.68	165
HLQR	11	5.69	1.66	6.21	15.18	90

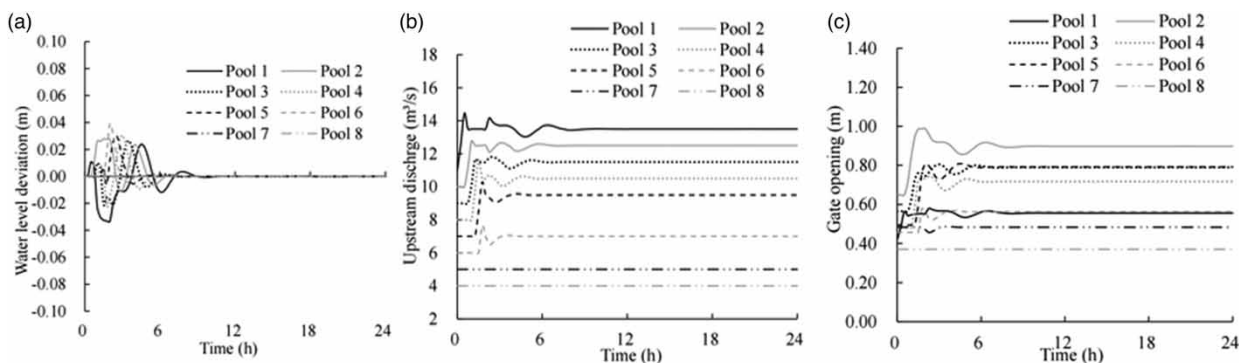
**Figure 7** | Multi-pool system control performance in test 2.

Table 5 | Control performance of multi-pool canal system

Control strategy	MAE (Max)	IAE (Average)	NIAQ (Average)	NIAW (Average)	Transition time (h) (Max)
Discharge compensation LQR ^a	8.89×10^{-2}	2.52×10^{-3}	8.50×10^{-4}	7.81×10^{-4}	21.50
The proposed HLQR	3.85×10^{-2}	3.32×10^{-4}	5.23×10^{-4}	2.37×10^{-4}	7.50
Improving	56.65%	87.18%	38.51%	69.69%	65.12%

Note that each canal system contained several pools, so statistics of each pool's indicators were collated to investigate the canal system's performance.

^aData from Zhong *et al.* (2020).

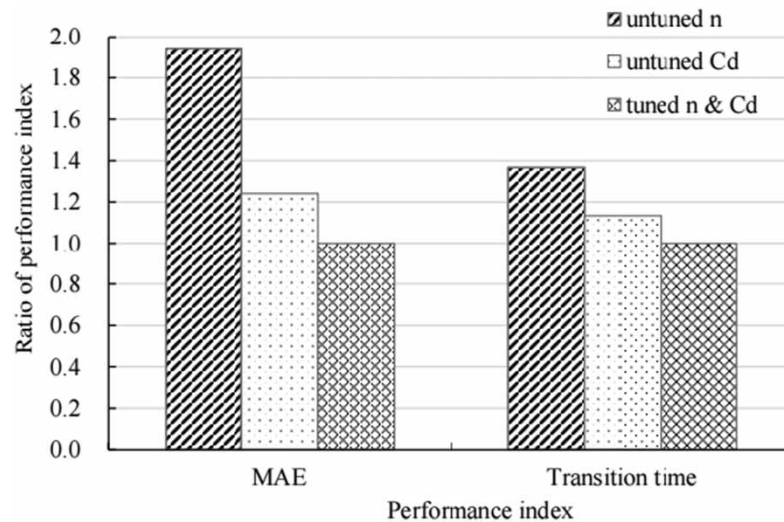
DCLQR generates a large number of control actions, contributing to the observed differences. Besides, the overall performance improvement can be attributed to the effective flow release managed by the feedforward component of HLQR, aided by model prediction, and the coordination between the feedforward and feedback of the hybrid controller.

4.4. Robust tests

As depicted in Figure 8 and summarized in Table 6, both indexes have increased compared to the well-tuned condition. With an untuned Manning n , the MAE of the water level is double that of the tuned condition. However, under the untuned C_d condition, the designed controller performs admirably in water level control, with only a 24% increase in MAE, which falls within a tolerable range. Moreover, there is no great increase in transition time. Even with a 20% error in n/C_d estimation, the HLQR controller can effectively handle the demand change, with an acceptable water level deviation and transition time.

5. DISCUSSION

In this paper, the ASCE canal serves as the study case under the designed controller across several scenarios. However, owing to variations in factors such as bed slope, side slope, roughness, etc., hydraulic responses may differ among different canals.

**Figure 8** | Multi-pool system control performance with untuned parameters.**Table 6** | Control performance of untuned discharge coefficient C_d and Manning n

Untuned parameter	MAE	Increase (%)	Transition time	Increase (%)
n (120%)	0.0747	94.03	10.25	36.67
C_d (120%)	0.0478	24.16	8.5	13.33

Consequently, in certain cases, calibration of IDZ model parameters becomes necessary, a process strongly linked to accuracy.

The concept behind the new controller draws inspiration from the integration of model prediction with optimal algorithms and the hybrid design employing LQR logic. In this controller structure, the proposed HLQR is not confined to the IDZ model; other canal models can be utilized as substitutes. However, one limitation lies in its high dependency on the accuracy of model prediction and the certainty of the delivery schedule. This challenge could potentially be addressed, in part, through the incorporation of incremental variables of states and actions (Horváth *et al.* 2015; Lemos & Sampaio 2015), as well as adaptive strategies (Tian *et al.* 2017; Liu *et al.* 2023).

When using LQR in canal control, the coefficients in weighting matrices are crucial to the results. Usually, two optimized quadratic performance indicators are taken from canal response characteristics and inherent design parameters of pools, which all are prior parameters, to determine weight matrices for evaluation objects (changes in water levels and flow rates). Zhong *et al.* (2020) propose a method called optimized quadratic performance indicators estimate (OQPIE) for the weight selection to provide satisfactory control effects of both water levels and flow rates, saving repeated tuning. This study is focused on the new hybrid controller and has only done some preliminary explorations in weighting coefficient determination. In the designed controller structure, the objective function in feedforward is allowed to be different from that in feedback. But we now just take the same weighting coefficients both in the feedforward and feedback controller and even in every pool of the canal system. The estimation and optimization of the weight matrix are beyond the scope of this article's research, and it is believed that the potential of the HLQR controller can be further explored with the help of optimization in the future.

When utilizing LQR in canal control, the coefficients in weighting matrices play a crucial role in the outcomes. Zhong *et al.* (2020) propose a method called OQPIE for weight estimation to achieve satisfactory control effects on both water levels and flow rates, thereby saving repeated tuning efforts. However, this study focuses on the new hybrid controller and makes limited explorations in weighting coefficient determination. In the designed controller structure, the objective function in feedforward is allowed to be different from that in feedback. However, currently, we adopt the same weighting coefficients for both the feedforward and feedback controllers and even for every pool of the canal system. The estimation and optimization of the cost weights are beyond the scope of this article's research. It is believed that the potential of the HLQR controller can be further explored with the help of optimization in the future.

6. CONCLUSION

This paper introduces a novel hybrid feedforward-feedback LQR controller based on model prediction, offering a simple and effective approach for routing known disturbances in open-channel systems and demonstrating satisfactory performance in constant water level control. The main conclusions are as follows:

- (1) The presented HLQR controller leads to fewer water level deviations and a shorter transition time for scheduled demand changes. Compared to DCLQR, improvements are observed in single-pool control, with a 19.90% decrease in MAE and a 55.36% reduction in IAE. Moreover, HLQR achieves a 40.03% reduction in transition time.
- (2) In multi-pool canal systems, the proposed controller exhibits comprehensive progress in water level deviation, control action cost, and transition speed. Compared to DCLQR, HLQR achieves a 56.65% reduction in MAE, saves 69.69% in gate movement, and reduces transition time from 21.5 to 7.5 h.
- (3) The designed controller demonstrates robustness with acceptable control performance when Manning's n and the coefficient of discharge C_d are untuned.

Future research avenues could explore diverse canal models, including high-order models and data-driven models, to serve as the prediction model in the hybrid configuration, thus enhancing prediction accuracy and controller performance. Additionally, field experiments should be conducted to validate the controller's effectiveness in practical control scenarios.

ACKNOWLEDGEMENTS

This work was financially supported by the National Natural Science Foundation of China (NSFC) under Grants (No. 51979202), and the National Key Research and Development Program (2022YFC3202504). We are grateful to the editors and the anonymous reviewers.

DATA AVAILABILITY STATEMENT

All relevant data are included in the paper or its Supplementary Information.

CONFLICT OF INTEREST

The authors declare there is no conflict.

REFERENCES

- Aguilar, J. V., Langarita, P., Linares, L. & Rodellar, J. (2009) Automatic control of flows and levels in an irrigation canal, *IEEE Transactions on Industry Applications*, **45** (6), 2198–2208. <https://doi.org/10.1109/tia.2009.2031941>.
- Askari Fard, A., Hashemy Shahdany, S. M. & Javadi, S. (2021) Automatic surface water distribution systems: a reliable alternative for energy conservation in agricultural section, *Sustainable Energy Technologies and Assessments*, **45**. <https://doi.org/10.1016/j.seta.2021.101216>.
- Askari Fard, A., Hashemy Shahdany, S. M., Javadi, S. & Maestre, J. M. (2022) Developing an automatic conjunctive surface-groundwater operating system for sustainable agricultural water distribution, *Computers and Electronics in Agriculture*, **194**.
- Aydin, B. E., van Overloop, P. J., Rutten, M. & Tian, X. (2017) Offset-free model predictive control of an open water channel based on moving horizon estimation, *Journal of Irrigation and Drainage Engineering*, **143** (3). [https://doi.org/10.1061/\(ASCE\)IR.1943-4774.0001085](https://doi.org/10.1061/(ASCE)IR.1943-4774.0001085).
- Balogun, O. S., Hubbard, M. & DeVries, J. J. (1998) Automatic control of canal flow using linear quadratic regulator theory, *Journal of Hydraulic Engineering*, **114** (1), 75–102.
- Bautista, E. & Clemmens, A. J. (2005) Volume compensation method for routing irrigation canal demand changes, *Journal of Irrigation and Drainage Engineering – ASCE*, **131** (6), 494–503. [https://doi.org/10.1061/\(ASCE\)0733-9437\(2005\)131:6\(494\)](https://doi.org/10.1061/(ASCE)0733-9437(2005)131:6(494)).
- Cantoni, M., Weyer, E., Li, Y., Ooi, S. K., Mareels, I. & Ryan, M. (2007) Control of large-scale irrigation networks, *Proceedings of the IEEE*, **95** (1), 75–91. <https://doi.org/10.1109/JPROC.2006.887289>.
- Clemmens, A. J. & Schuurmans, J. (2004) Simple optimal downstream feedback canal controllers: theory, *Journal of Irrigation and Drainage Engineering*, **130** (1), 26–34. [https://doi.org/10.1061/\(ASCE\)0733-9437\(2004\)130:1\(26\)](https://doi.org/10.1061/(ASCE)0733-9437(2004)130:1(26)).
- Clemmens, A. J. & Wahlin, B. T. (2004) Simple optimal downstream feedback canal controllers: ASCE test case results, *Journal of Irrigation and Drainage Engineering*, **130** (1), 35–46. [https://doi.org/10.1061/\(ASCE\)0733-9437\(2004\)130:1\(35\)](https://doi.org/10.1061/(ASCE)0733-9437(2004)130:1(35)).
- Clemmens, A. J., Kacerek, T. F., Grawitz, B. & Schuurmans, W. (1998) Test cases for canal control algorithms, *Journal of Irrigation and Drainage Engineering*, **124** (1), 23–30. [https://doi.org/10.1061/\(ASCE\)0733-9437\(1998\)124:1\(23\)](https://doi.org/10.1061/(ASCE)0733-9437(1998)124:1(23)).
- Clemmens, A. J., Strelkoff, T. S. & Replogle, J. A. (2003) Calibration of submerged radial gates, *Journal of Hydraulic Engineering*, **129** (9), 680–687. [https://doi.org/https://doi.org/10.1061/\(ASCE\)0733-9429\(2003\)129:9\(680\)](https://doi.org/https://doi.org/10.1061/(ASCE)0733-9429(2003)129:9(680)).
- Clemmens, A. J., Strand, R. J. & Bautista, E. (2010) Routing demand changes to users on the WM lateral canal with sacMan, *Journal of Irrigation and Drainage Engineering*, **136** (7), 470–478. [https://doi.org/10.1061/\(ASCE\)IR.1943-4774.0000226](https://doi.org/10.1061/(ASCE)IR.1943-4774.0000226).
- Conde, G., Quijano, N. & Ocampo-Martinez, C. (2021) Modeling and control in open-channel irrigation systems: a review, *Annual Reviews in Control*, **51**, 153–171. <https://doi.org/10.1016/j.arcontrol.2021.01.003>.
- Cunge, J. A., Holly, F. M. & Verwey, A. (1980) *Practical Aspects of Computational River Hydraulics*.
- Dent, P. (2004). 'Submerged radial gate calibration using historical data to improve canal automation performance', *Proc., Proceedings of the 2004 World Water and Environmental Resources Congress: Critical Transitions in Water and Environmental Resources Management*, pp. 2244-2250.
- Dorf, R. C. & Bishop, R. H. (2016) *Modern Control Systems*. Pearson Education.
- Garg, N. K. & Dadhich, S. M. (2014) Integrated non-linear model for optimal cropping pattern and irrigation scheduling under deficit irrigation, *Agricultural Water Management*, **140**, 1–13. <https://doi.org/10.1016/j.agwat.2014.03.008>.
- Gerbeau, J.-F. & Perthame, B. (2021) Derivation of viscous Saint-Venant system for laminar shallow water; numerical validation, *Discrete and Continuous Dynamical Systems – Series B*, **1** (1), 89–102.
- Godfray, H. C. J., Beddington, J. R., Crute, I. R., Haddad, L., Lawrence, D., Muir, J. F., Pretty, J., Robinson, S., Thomas, S. M. & Toulmin, C. (2010) Food security: the challenge of feeding 9 billion people, *Science*, **327** (5967), 812–818. <https://doi.org/10.1126/science.1185385>.
- Guanghua, G., Ke, Z., Wenjun, L., Changcheng, X. & Haiwang, S. (2018) Optimization of controller parameters based on nondimensional performance indicators for canal systems, *Transactions of the Chinese Society of Agricultural Engineering*, **34** (7), 90–99. <https://doi.org/10.11975/j.issn.1002-6819.2018.07.012>.
- Hashemy Shahdany, S. M., Taghvaeian, S., Maestre, J. M. & Firoozfar, A. R. (2019) Developing a centralized automatic control system to increase flexibility of water delivery within predictable and unpredictable irrigation water demands, *Computers and Electronics in Agriculture*, **163**. <https://doi.org/10.1016/j.compag.2019.104862>.
- Horváth, K., Galvis, E., Valentín, M. G. & Rodellar, J. (2015) New offset-free method for model predictive control of open channels, *Control Engineering Practice*, **41**, 13–25. <https://doi.org/10.1016/j.conengprac.2015.04.002>.
- Kacerek, T. F., Clemmens, A. & Sanfilippo, F. 'Test cases for canal control algorithms with examples', *Proc., International Water Resources Engineering Conference – Proceedings*, pp. 184-188.

- Kong, L., Yang, Q., Chen, R., Zhang, Z., Li, Y. & Shi, Y. (2024) Improved proportional integral (PI) controller for water level control in open channel systems: a case study of the middle route project for south-to-north water transfer, *Journal of Hydrology: Regional Studies*, **51**. <https://doi.org/10.1016/j.ejrh.2023.101646>.
- Kurganov, A. & Levy, D. (2002) Central-Upwind schemes for the Saint-Venant System, *ESAIM: Mathematical Modelling and Numerical Analysis*, **36** (3), 397–425. <https://doi.org/10.1051/m2an:2002019>.
- Lemos, J. M. & Sampaio, I. (2015) Distributed LQG control for multiobjective control of water canals, *Operations Research/Computer Science Interfaces Series*, 59–73.
- Litrico, X. & Fromion, V. (2004a) Analytical approximation of open-channel flow for controller design, *Applied Mathematical Modelling*, **28** (7), 677–695. <https://doi.org/10.1016/j.apm.2003.10.014>.
- Litrico, X. & Fromion, V. (2004b) Frequency modeling of open-channel flow, *Journal of Hydraulic Engineering*, **130** (8), 806–815. [https://doi.org/10.1061/\(ASCE\)0733-9429\(2004\)130:8\(806\)](https://doi.org/10.1061/(ASCE)0733-9429(2004)130:8(806)).
- Litrico, X. & Fromion, V. (2004c) Simplified modeling of irrigation canals for controller design, *Journal of Irrigation and Drainage Engineering*, **130** (5), 373–383.
- Litrico, X. & Fromion, V. (2006) Boundary control of linearized Saint-Venant equations oscillating modes, *Automatica*, **42** (6), 967–972. <https://doi.org/10.1016/j.automatica.2006.02.002>.
- Litrico, X. & Fromion, V. (2009) *Modeling and Control of Hydrosystems*. Springer, pp. 1-409.
- Liu, J., Wang, Z., Yang, Z. & Zhang, T. (2023) An adaptive predictive control algorithm for comprehensive dendritic canal systems, *Journal of Irrigation and Drainage Engineering*, **149** (1). [https://doi.org/10.1061/\(ASCE\)IR.1943-4774.0001736](https://doi.org/10.1061/(ASCE)IR.1943-4774.0001736).
- Liu, W., Guan, G., Tian, X., Cao, Z., Chen, X. & Shi, L. (2024) A real-time refined roughness estimation framework for the digital twin model calibration of irrigation canal systems, *Journal of Irrigation and Drainage Engineering*, **150** (1). <https://doi.org/10.1061/jidedh.Ireng-10227>.
- Malaterre, P. O. (1995) Regulation of irrigation canals – characterisation and classification, *Irrigation and Drainage Systems*, **9** (4), 297–327. <https://doi.org/10.1007/BF00881619>.
- Malaterre, P. O. (2008). 'Control of irrigation canals: why and how?', *Proc., Proceedings of the International Workshop on Numerical Modelling of Hydrodynamics for Water Resources – Numerical Modelling of Hydrodynamics for Water Resources*, pp. 271–292.
- Rabbani, T., Munier, S., Dorchies, D., Malaterre, P.-O., Bayen, A. & Litrico, X. (2009) Flatness-based control of open-channel flow in an irrigation canal using SCADA, *IEEE Control Systems*, **29** (5), 22–30. <https://doi.org/10.1109/MCS.2009.933524>.
- Scokaert, P. O. M. & Rawlings, J. B. (1998) Constrained linear quadratic regulation, *IEEE Transactions on Automatic Control*, **43** (8), 1163–1169. <https://doi.org/10.1109/9.704994>.
- Shen, W., Chen, X., Pons, M. N. & Corriou, J. P. (2009) Model predictive control for wastewater treatment process with feedforward compensation, *Chemical Engineering Journal*, **155** (1–2), 161–174. <https://doi.org/10.1016/j.cej.2009.07.039>.
- Tian, X., Negenborn, R. R., van Overloop, P. J., María Maestre, J., Sadowska, A. & van de Giesen, N. (2017) Efficient multi-scenario model predictive control for water resources management with ensemble streamflow forecasts, *Advances in Water Resources*, **109**, 58–68. <https://doi.org/10.1016/j.advwatres.2017.08.015>.
- Tork, H., Javadi, S. & Hashemy Shahdany, S. M. (2021) A new framework of a multi-criteria decision making for agriculture water distribution system, *Journal of Cleaner Production*, **306**. <https://doi.org/10.1016/j.jclepro.2021.127178>.
- van Overloop, P.-J., Weijs, S. & Dijkstra, S. (2008) Multiple model predictive control on a drainage canal system, *Control Engineering Practice*, **16** (5), 531–540. <https://doi.org/10.1016/j.conengprac.2007.06.002>.
- Vorosmarty, C. J., McIntyre, P. B., Gessner, M. O., Dudgeon, D., Prusevich, A., Green, P., Glidden, S., Bunn, S. E., Sullivan, C. A., Liermann, C. R. & Davies, P. M. (2010) Global threats to human water security and river biodiversity, *Nature*, **467** (7315), 555–561. <https://doi.org/10.1038/nature09440>.
- Wakamori, K., Mizuno, R., Nakanishi, G. & Mineno, H. (2020) Multimodal neural network with clustering-based drop for estimating plant water stress, *Computers and Electronics in Agriculture*, **168**. <https://doi.org/10.1016/j.compag.2019.105118>.
- Wang, C. D. & Guan, G. H. (2011) *Simulation and Control of Canal System*. China.
- Weyer, E. (2008) Control of irrigation channels, *IEEE Transactions on Control Systems Technology*, **16** (4), 664–675. <https://doi.org/10.1109/TCST.2007.912122>.
- Yang, Q., Kong, L., Song, P., Lei, X. & Wang, H. (2020) Study on linear optimal control method of open canal flows coupled with feedforward control strategy, *Journal of Hydroelectric Engineering/Shuilifadianxuebao*, **39** (05), 64–71. <https://doi.org/10.11660/slfdx.20200506>.
- Zhong, K., Guan, G., Tian, X., Maestre, J. M. & Mao, Z. (2020) Evaluating optimization objectives in linear quadratic control applied to open canal automation, *Journal of Water Resources Planning and Management*, **146** (11). [https://doi.org/10.1061/\(asce\)wr.1943-5452.0001286](https://doi.org/10.1061/(asce)wr.1943-5452.0001286).
- Zhu, Z., Guan, G. & Wang, K. (2023) Distributed model predictive control based on the alternating direction method of multipliers for branching open canal irrigation systems, *Agricultural Water Management*, **285**. <https://doi.org/10.1016/j.agwat.2023.108372>.

First received 10 July 2024; accepted in revised form 20 November 2024. Available online 11 December 2024